

Supporting Information

Polymerization of N-acryloylsemicarbazide: A Facile and Versatile Strategy to Tailor-Make Highly Stiff and Tough Hydrogels

Chuanchuan Fan, Bo Liu, Ziyang Xu, Chunyan Cui, Tengling Wu, Yang Yang, Dongfei Zhang, Meng Xiao, Zhuodan Zhang, Wenguang Liu*

School of Materials Science and Engineering, Tianjin Key Laboratory of Composite and Functional Materials,

Tianjin University, Tianjin 300350, China

*Corresponding author (E-mail: wgliu@tju.edu.cn)

EXPERIMENTAL SECTION

Materials. Semicarbazide hydrochloride (98%, Energy Chemical, Shanghai, China), acryloyl chloride (98%, TCI, Shanghai, China), diethyl ether (Yuanli Company, Tianjin, China), 2-hydroxy-2-methyl-1-propanone (IRGACURE 1173, 98%, Sigma-Aldrich) N-(3-aminopropyl) methacrylamide hydrochloride (APMAm, 98%, Heowns Company, Tianjin, China), 1-ethyl-3-(3-dimethylaminopropyl) carbodiimide hydrochloride (EDC, 98%, Heowns Company, Tianjin, China), N-hydroxysuccinimide (NHS, Heowns Company, Tianjin, China) were used as received. N-acryloyl glycinamide (NAGA) was synthesized according to the protocol reported in our previous study.¹ All other chemical reagents were of analytical grade.

Synthesis of N-acryloylsemicarbazide (NASC). Semicarbazide hydrochloride (12.7 g), 12 mL deionized water, 67.2 mL of cool K₂CO₃ solution (2 M) and 36 mL cold diethyl ether were successively added into a 250 mL round-bottom flask. Then, 11.4 g of acryloyl chloride in 48 mL diethyl ether was added dropwise to the above solution under stirring at 0 °C for about 30 min. After that, the mixture was continuously stirred for 4 h at the same temperature. After that, the white

precipitate formed was collected by filtration, and washed by cold water to achieve crude product. The crude product was dissolved in deionized and distilled water and stirred for 3 h at 95 °C. Subsequently, the undissolved precipitate was removed by centrifuge, and the supernatant was freeze-dried to obtain final NASC monomer.

Figure S1 and **Figure S2** show ^1H NMR and ^{13}C NMR spectrum of NASC, respectively. ^1H NMR (400 MHz, DMSO- d_6): δ = 9.63 (H_a , -NH-NH-), 7.78 (H_b , -NH-NH-), 6.21 (H_c , -CH₂-CH-), 6.21 and 5.66 (H_e , -CH₂-CH-), 5.78 (H_d , -NH₂). ^{13}C -NMR (400 MHz, DMSO- d_6): δ = 164.6 (C_a , -CO-), 158.9 (C_b , -CO-), 130.3 (CH₂-CH-), 126.3 (CH₂-CH-). **Figure S3** displays feature bands of NASC: FTIR (cm^{-1}): 3443 (NH), 3322 (NH), 3217 (NH), 3054 (NH), 1682 (C=O), 1624 (C=C), 1597 (NH).

Synthesis of Heparin Methacrylamide (HepMAM). 1.0 g of heparin and 0.25 g of APMAM were dissolved in 150 mL 4-morpholineethanesulfonic acid hydrate (MES) buffer (0.05 M, pH 5.3, 0.1 M NaCl). Then 0.96 g EDC and 0.29 g NHS were added, and stirred at 25 °C for 24 h. NaCl and cold ethanol were sequentially added into the above mixture. The white precipitate was obtained after centrifugation and was re-dissolved in deionized and distilled water. Finally, the aqueous solution was dialyzed, lyophilized, and the product was stored at -20 °C until use. **Figure S16** shows ^1H NMR spectrum of HepMAM. The peaks at 5.69 and 5.44 ppm confirm the existence of a C=C, indicating the successful synthesis of HepMAM.

Synthesis of Poly(N-acryloylsemicarbazide) (PNASC) Hydrogels and PNASC Copolymers. A certain mass of the monomer NASC was dissolved in a mixed solvent of DMSO and water (7/3, v/v) according to the desired recipes, and then 1 wt% of photoinitiator IRGACURE 1173 (relative to total of NASC) was added and further stirred until they were completely dissolved under N₂ atmosphere. The mixture was cast into PMMA molds and polymerization was carried out for 60 min in a crosslink

oven (XL-1000 UV Crosslinker, Spectronics Corporation, NY, USA). The obtained gels were thoroughly washed with deionized water to completely remove DMSO. A series of PNASC hydrogels were prepared by varying initial monomer concentration and were named as PNASC-X (X denoted volume percentage concentration). A band at 1624 cm^{-1} disappears in the FTIR spectrum (**Figure S3**) after photopolymerization, indicating the occurrence of polymerization reaction. In the same way, copolymer hydrogels of NASC with AAm, CBAA and HepMAm were respectively prepared and named as P(NASC-co-AAm)-M (M denoted volume percentage concentration; the weight ratio of NASC and AAm was 2/1; the volume ratio of DMSO and H_2O was 7/3), P(NASC-co-CBAA)-N (N denoted volume percentage concentration; the weight ratio of NASC and CBAA was 2/1; the volume ratio of DMSO and H_2O was 3/7), and P(NASC-co-HepMAm)-25-Y (25 denoted volume percentage concentration of NASC; Y denotes mass concentration in mg/mL). PNAGA-25 (25 denoted volume percentage concentration) was synthesized according to the protocol reported in our previous study.¹

Measurement of Molecular Weight of PNASC. The molecular weight of PNASC was measured by gel permeation chromatography (GPC, Waters Styragel columns and a Water-2414 refractive index detector) at $40\text{ }^{\circ}\text{C}$. DMSO was used as the eluent with a flow rate of 1.0 mL min^{-1} . The number average molecular weight (M_n) and polydispersity were determined to be 161,000 and 1.2, respectively.

Measurement of Transmittance of PNASC Gels. The transparency of PNASC gels was measured on a UV-vis spectrophotometer (TU-1810, China) at room temperature at a wavelength of 600 nm.

X-ray Diffraction (XRD) Measurement. XRD patterns of the hydrogels were recorded using D8 Advanced (Bruker, Germany). XRD data were obtained from 5° to 50° (2θ) using $\text{Cu K}\alpha$ radiation with a scan rate of $1^{\circ}\text{ min}^{-1}$.

Small-angle X-ray Scattering (SAXS) Measurement. SAXS measurements were carried out at

room temperature on the BL16B1 beamline of Shanghai Synchrotron Radiation Facility (SSRF). The wavelength of radiation source is 0.124 nm. Two-dimensional (2D) patterns were collected by a Pilatus 2M detector with 1475×1679 pixels and a pixel size of $172 \mu\text{m} \times 172 \mu\text{m}$ and the distance of the sample to detector is 1880 mm.

Measurement of Mechanical Properties. The mechanical properties of the hydrogels were tested on Instron 2344 Microtester in a water bath at 25 °C unless otherwise stated. All the hydrogels after swelling equilibrium were cut into dumbbell shaped specimens according to ASTM standard. The stretching rate of tensile test and loading-unloading test was fixed at 50 mm min⁻¹. The stress of the hydrogel sample was obtained using the following formula:

$$\sigma = F/A \quad (\text{S1})$$

where F and A are the applied load and the initial cross-sectional area, respectively.

For tearing test, the hydrogel samples were cut into trouser shape with an initial notch length 20 mm, and the two arms were firmly clamped to the tester with the tensile test rate of 50 mm min⁻¹. The fracture energy was calculated as:

$$\Gamma = \frac{2F_{ave}}{d} \quad (\text{S2})$$

Where F_{ave} and d are the average load during the tear and the thickness of samples respectively.

Rheology Test of the Hydrogels. Rheological behaviors of the hydrogels were measured using a rheometer (MCR 302, Austria) equipped with a plate with a diameter of 25 mm and Peltier device for temperature control. The hydrogel samples were cut into disc-shapes (25 mm in diameter and ~1 mm in thickness), and were adhered to the plates and surrounded by silicone oil. Temperature sweep was performed to the sample from 20 to 90 °C (heating rate: 5 °C/min) at a strain amplitude of 0.05% (in the linear region) and a frequency of 1 Hz.

Dynamic Light Scattering (DLS) Measurement. The difference in hydrodynamic size of PNASC-0.5 and PNAGA-0.5 was monitored by DLS using Malvern Zetasizer Nano ZS instrument.

Dynamic Mechanical Analysis (DMA). The hydrogel samples were cut into rectangle shapes (30 mm in length and 5 mm in width). G' and G'' of the hydrogels were measured on a TA Q800 Dynamic Mechanical Analyzer at 1 Hz in a temperature range of 10-63 °C in pure water with heating rate of 2 °C min⁻¹.

Computer Simulation Test. The geometry optimization was performed with Gaussian 09 software. The model was optimized by B3LYP/6-31G(d,p). The polarizable continuum model was applied to consider the solvent water environmental effect. With the optimized structure, the hydrogen bonding interaction energy was evaluated by the Fragment Molecular Orbital Method (FMO).

Measurement of Nonspecific Protein Adsorption. Evaluation of the protein adsorption was carried out by a procedure adapted from our previous report.²

Cytotoxicity Assay of Hydrogels. The assay was referred to the protocol reported previously.³

Hemolysis Assay. Fresh blood was obtained from a rabbit, whose red blood cells (RBCs) were separated by centrifugation at 5000 rpm for 5 min, washed five times with phosphate-buffered saline (PBS, pH 7.4). The diluted RBC suspension was incubated with the hydrogel disks (PNASC-25, P(NASC-co-HepMAM)-25-Y). Deionized water-dispersed RBCs were used as the positive control, and the PBS (pH 7.4)-dispersed RBCs were used as the negative control. All suspensions were incubated at 37 °C for 2 h and then centrifuged at 5000 rpm for 3 min. The supernatants were transferred to a 48-well plate. The optical absorbance of each well was measured on a Σ 960 plate-reader (Meter-tech) at the wavelength of 540 nm. The hemolysis ratio was calculated using the following formula.⁴

$$\text{HR (\%)} = \frac{\text{suspensionsabs} - \text{negative controlabs}}{\text{positive controlabs} - \text{negative controlabs}} \times 100\%$$

(S3)

Measurement of Burst Pressure. The burst pressure was measured on Instron 2344 Microtester in a water bath at 25 °C unless otherwise stated. The hydrogel tubes (1.5 mm diameter, 10 mm length and 0.5 mm thickness of tube wall) were used for burst pressure test (n=3). The hydrogel tube was fixed to the tenser by two L-shaped clamps according to the reported method.⁵ A rate of 0.6 mm min⁻¹ was applied to the sample. The ultimate circumferential tensile strength (UCTS) was defined as the maximum stress reached before sample fractured. The burst pressure of the tube was estimated from the UCTS values by adaptation of Laplace's law for intraluminal pressure:⁶

$$\text{Burst pressure (mmHg)} = (\text{UCTS} \times d)/R_0 \quad (\text{S4})$$

where d and R₀ were the thickness of the tube and the intraluminal radius of the tube at atmospheric pressure respectively.

Measurement of Suture Retention Strength. The hydrogel films were cut into rectangle shapes (5-mm width, 10-mm length, and 0.5-mm thickness). One end of the membrane was fixed to the clamp of the tester and the other side was connected to another clamp by 5-0 prolene. The suture was placed 2 mm from the edge of the hydrogel. The distance of the clamps was 1.5 cm. The test was carried out with the speed of 50 mm/min until the hydrogel film was fractured. Suture retention strength was defined as fracture strength.⁶

***In Vitro* Antithrombotic Test.** Antithrombotic behavior of the hydrogels sheets was tested using whole blood according to reported method.⁷ In short, the PNASC-25, P(NASC-co-HepMAM)-25-10 and P(NASC-co-HepMAM)-25-15 sheets were immersed in fresh whole blood for 12 h at room temperature. The hydrogel sheets were then washed with PBS buffer, followed by fixation with

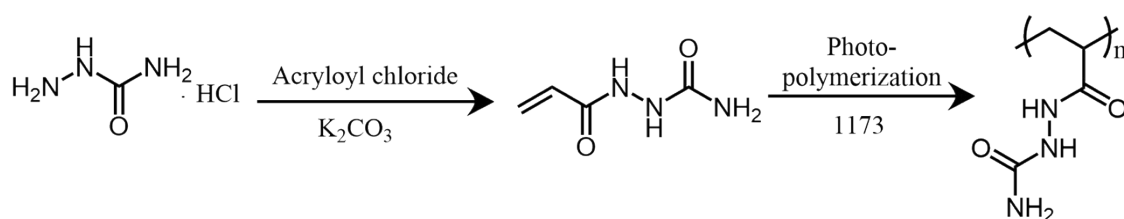
glutaraldehyde. After being dehydrated using gradient ethanol and vacuum drying, all sheets were coated with gold by a sputter coater for 45 s for SEM analysis. The sheets were observed by a field emission scanning electron microscope (FE-SEM, SU1510, Japan) at accelerated electron energy of 5.0 kV.

Subcutaneous Implantation. All the animal experiments were conducted in accordance with the guidelines of the Council for the Purpose of Control and Supervision of Experiments on Animals, Ministry of Public Health, China. The animal experiments were approved by the Animal Ethical Committee of Tianjin Institute of Medical and Pharmaceutical Science, China. The *in vivo* biocompatibility of the hydrogels was assayed by implanting the hydrogel disks into the subcutaneous tissues of mice for 4 weeks. Then, the mice were killed at predetermined intervals. The implanted materials and the surrounding tissues were removed and analyzed by histological staining. The biocompatibility was studied by hematoxylin and eosin staining.

Graft Implantation and Postoperative Observations: Adult male rabbits weighing 2.5-3 kg were used for evaluating the performance of the hydrogel artificial blood vessel. The PNASC-25 and P(NASC-co-HepMAM)-25-15 hydrogel tubes (1.5 mm in diameter, 2.5 cm in length) were separately implanted into the left carotid artery, respectively (five rabbits per group). Before surgery, the rabbits were anesthetized via an auricular vein injection of sodium pentobarbital solution (35 mg kg⁻¹) and heparin (100 Units/kg) was injected as an anti-coagulant agent. The rabbits were fixed on an operating table, and the neck skin was shaved and disinfected. The skin was cut with a scalpel, and the muscle was blunt-dissected by a hemostatic forcep to expose the left common carotid artery. The left common carotid artery was isolated, clamped, and transected. A hydrogel tube was inserted into the two ends of the blood vessel and fixed by surgical suture. Four hours after implantation, the hydrogel tube was removed, rinsed with saline solution. The hydrogel tubes were observed under a stereomicroscope

(NIKON SMZ 745T, Japan). At the designated time point (0 h, 1 h, 2 h, 4 h), the antithrombotic behavior was evaluated by changes of the blood color.

Statistical Analysis: *In vitro* experiments were analyzed by the one-way analysis of variance (ANOVA) with Tukey' post hoc test and expressed as means \pm standard deviations (SD). Statistical significance was defined as having $*P < 0.05$. SPSS 20.0 was used for statistical analysis of data.



Scheme S1. Synthesis of NASC and PNASC.

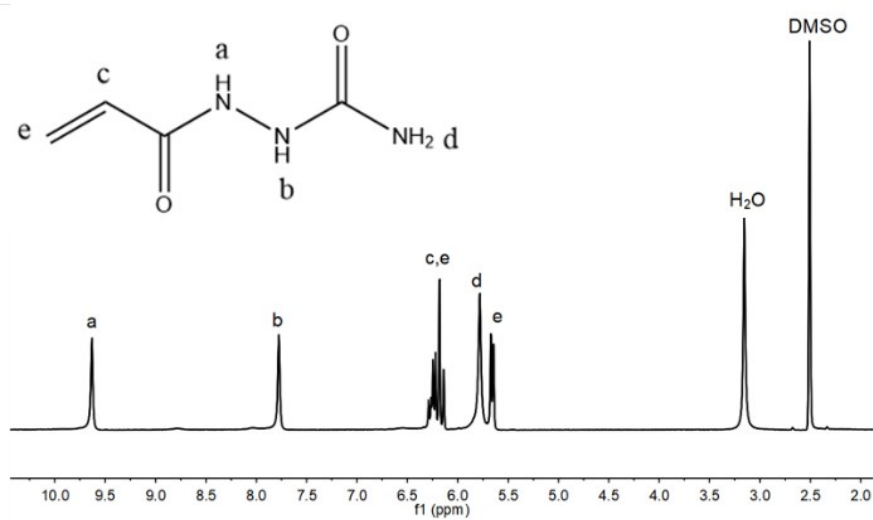


Figure S1. ¹H NMR spectrum of NASC in DMSO-d₆.

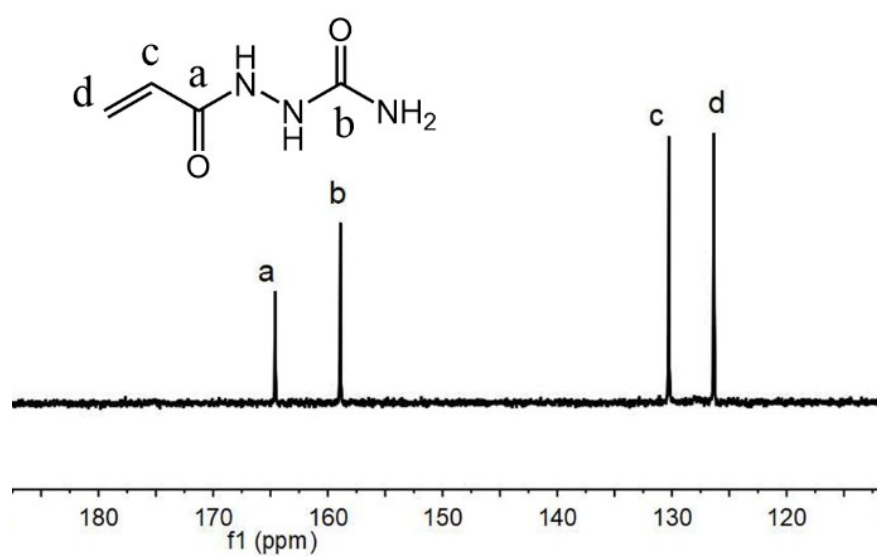


Figure S2. ^{13}C NMR spectrum of NASC in DMSO-d_6 .

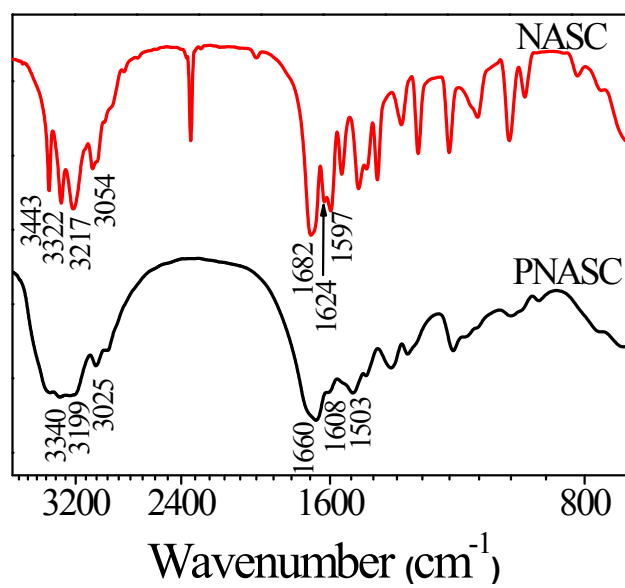


Figure S3. FTIR spectra of NASC and PNASC.

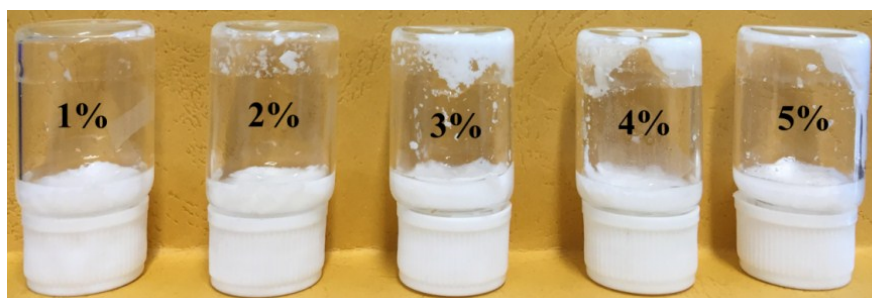


Figure S4. Photographs of PNASC prepared from varied monomer concentrations in an aqueous solution. Numbers in the images are initial volume percentage concentration of NASC.

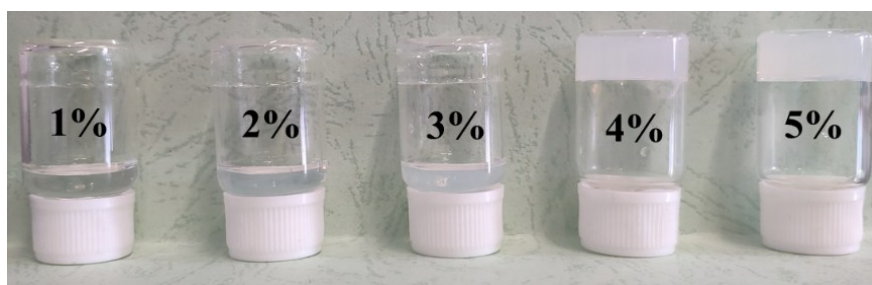


Figure S5. Photographs of PNASC hydrogels prepared from varied monomer concentrations in a mixture of DMSO/H₂O solution. Numbers in the images are initial volume percentage concentration of NASC.

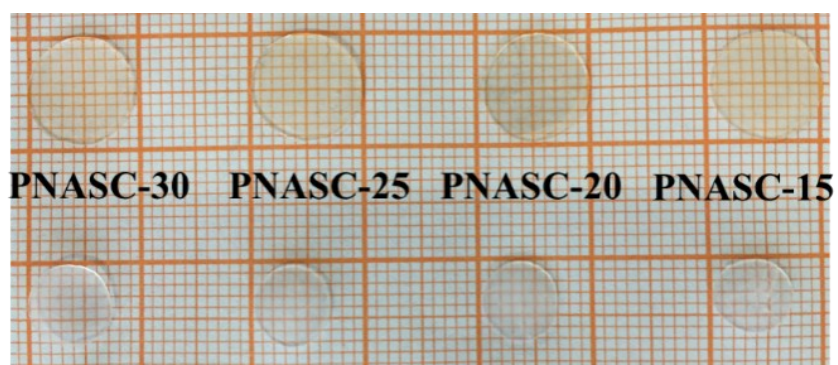


Figure S6. Photos of the PNASC gels immersed in water for 10 days.

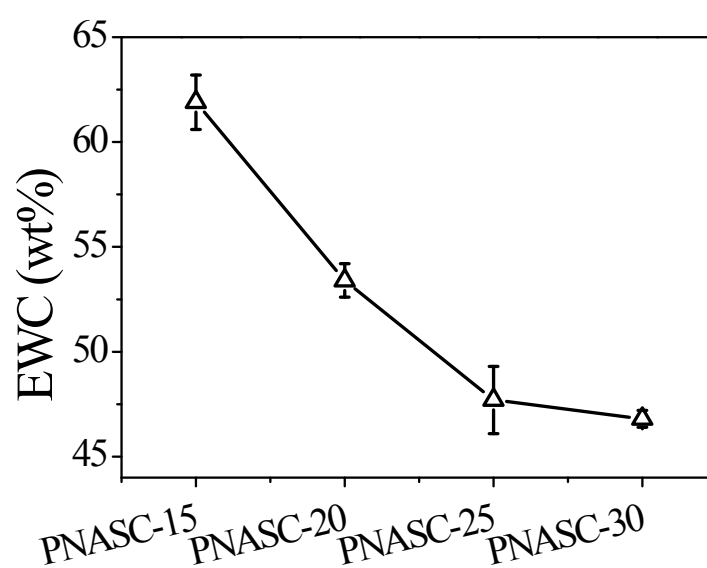
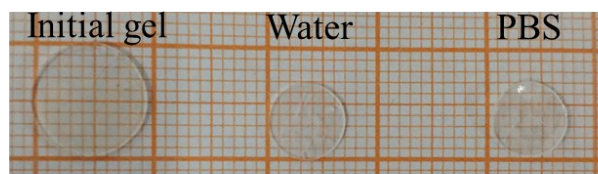


Figure S7. Effect of the monomer concentration on the EWCs of PNASC hydrogels.

a



b

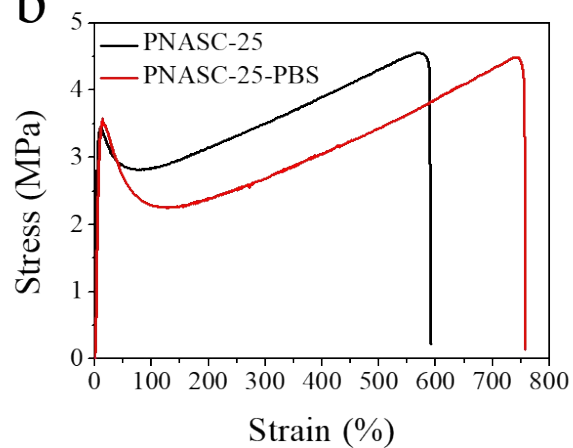


Figure S8. Photo (a), tensile stress-strain curves (b) of representative PNASC-25 gel immersing in water and PBS for 10 days, respectively. PNASC-25 and PNASC-25-PBS refer to the PNASC-25 gel soaked in water and PBS for 10 days, respectively.

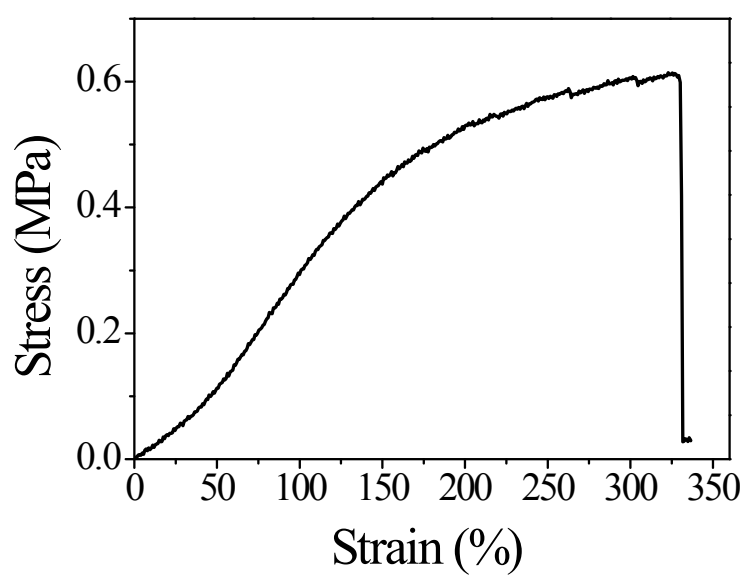


Figure S9. Tensile stress-strain curve of the as-prepared PNASC-25 gel before water exchange to form a hydrogel.

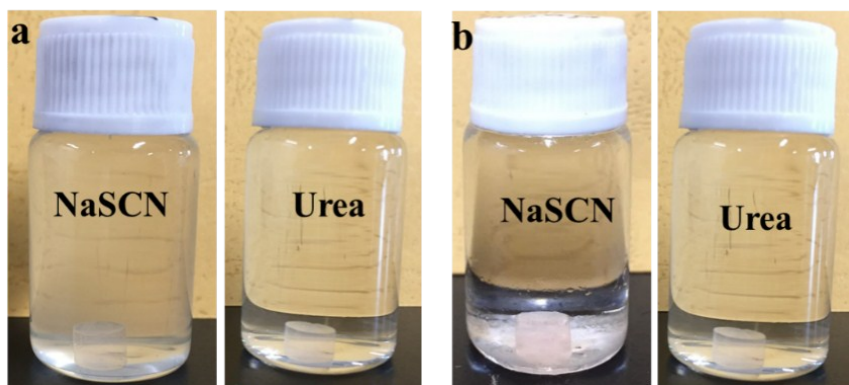


Figure S10. Swelling stability of the hydrogels at different immersion times. PNASC-25 hydrogel in 5 mol L⁻¹ NaSCN solution and in 5 mol L⁻¹ urea solution at room temperature for 0 h (a) at 90 °C for 12 h (b).

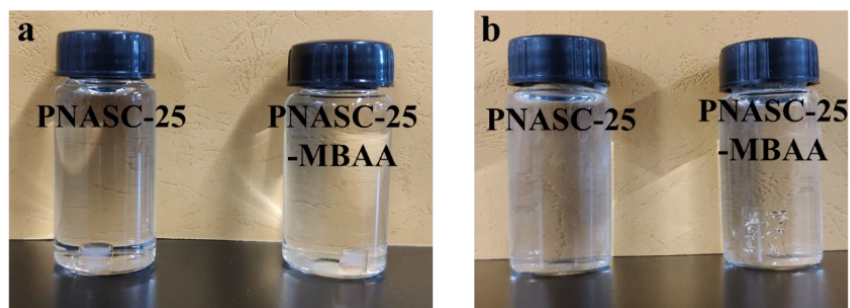


Figure S11. Swelling stability of the hydrogels at different immersion times. PNASC-25 hydrogel and MBAA-crosslinked PNASC-25 hydrogel (PNASC-25-MBAA) were respectively immersed in NaOH/urea solution (8 g of NaOH and 4 g urea in 100 mL water) at room temperature for 0 h (a) and 5 days (b).

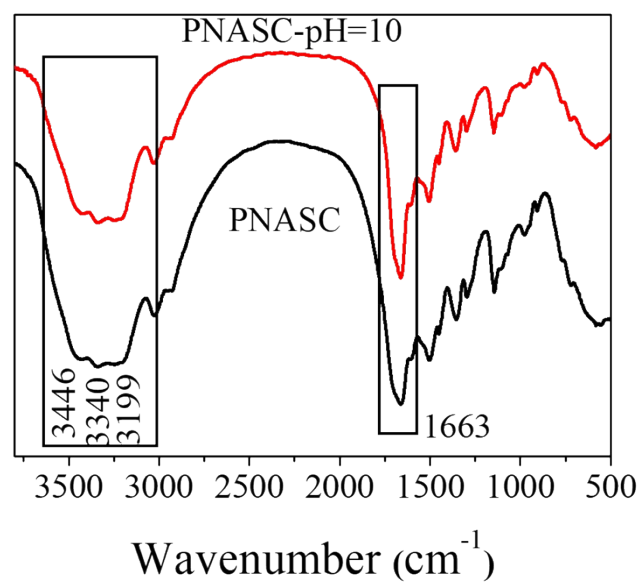


Figure S12. FTIR spectra of PNASC-25 and PNASC-pH=10 hydrogel. PNASC-pH=10 hydrogel denotes the PNASC-25 hydrogel that was first soaked in a medium of pH=10 and then was replaced with water to remove NaOH. After that the hydrogel was freeze-dried for FTIR measurement.

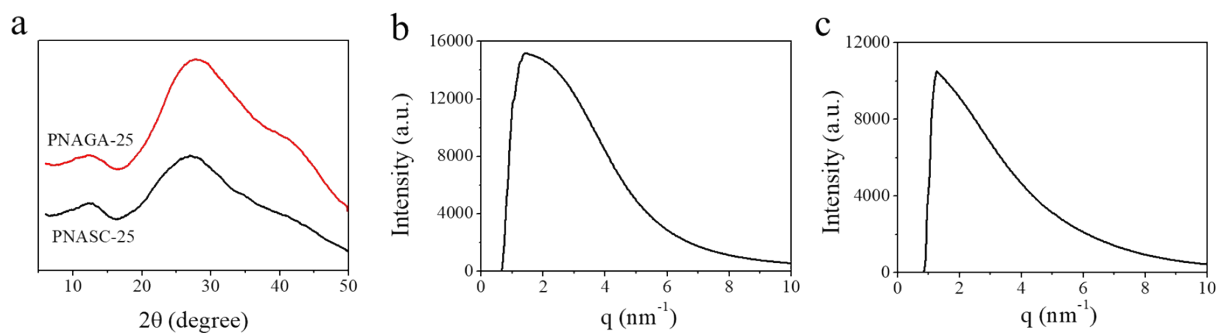


Figure S13. (a) XRD patterns of PNAGA-25 and PNASC-25 hydrogels. (b) and (c) are SAXS patterns of PNASC-25 and PNAGA-25 hydrogels, respectively.

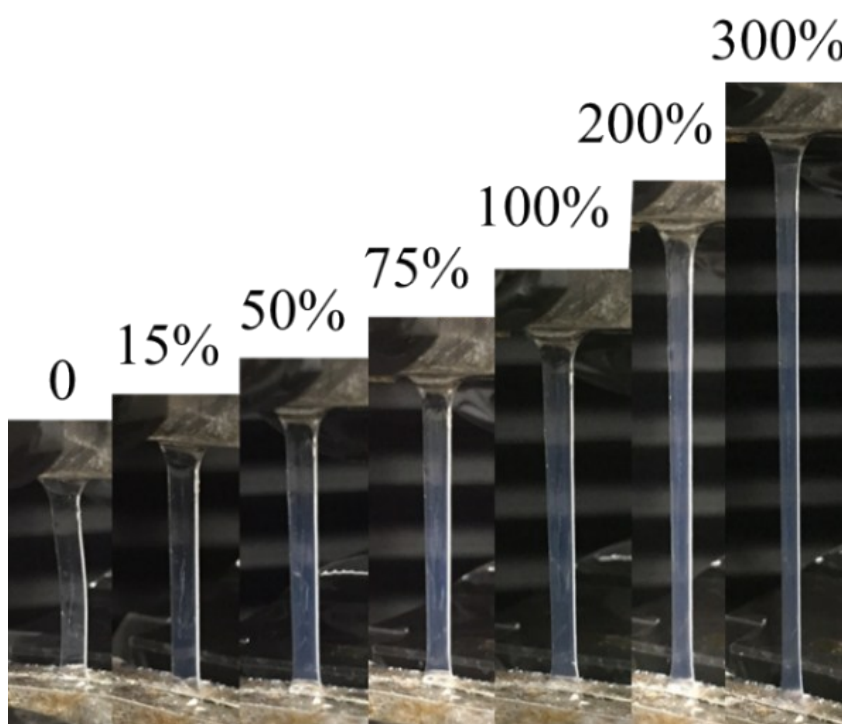


Figure S14. Photos of PNASC-25 hydrogel recorded during stretching.

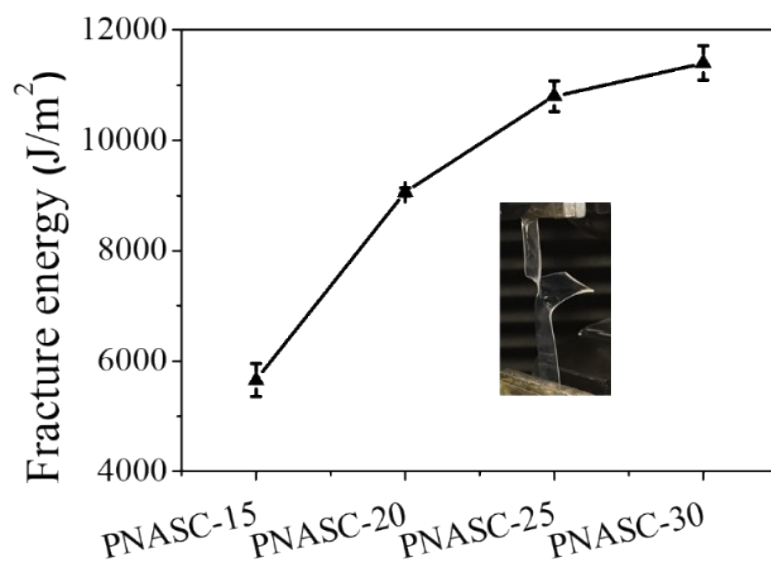


Figure S15. Fracture energies of PNASC hydrogels prepared with various initial monomer concentrations. Inset showing the tearing test of trouser shaped PNASC-25 hydrogel on the tester.

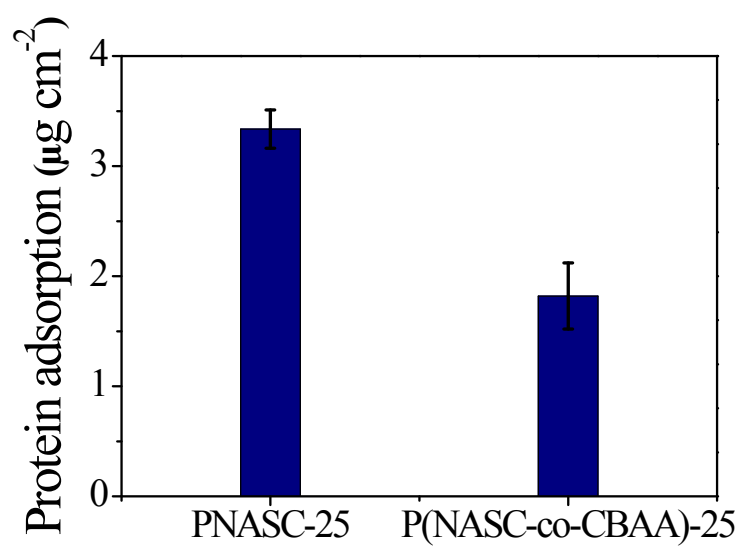


Figure S16. Protein adsorption on PNASC-25 and P(NASC-co-CBAA) hydrogels. The P(NASC-co-CBAA) hydrogel exhibits much lower protein adsorption compared to PNASC hydrogel.

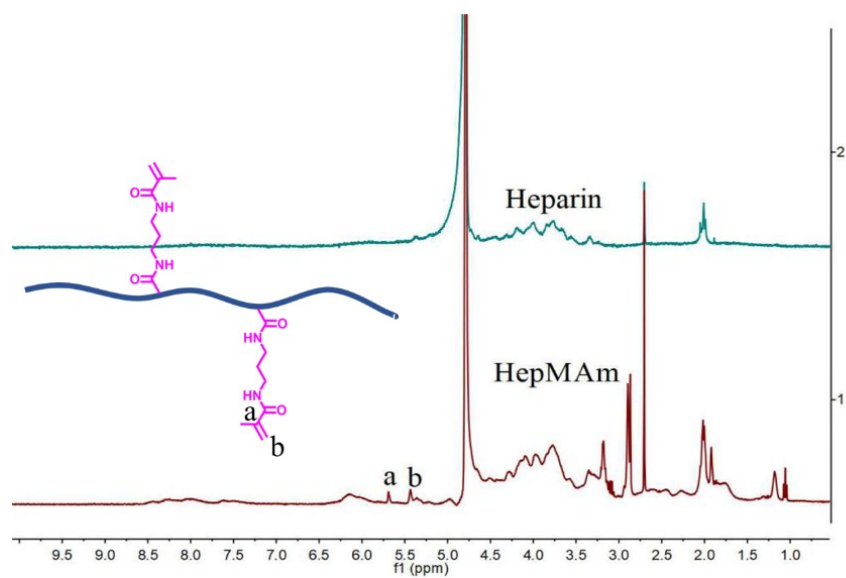


Figure S17. ^1H NMR spectra of heparin and HepMAM in D_2O . The peaks at 5.69 and 5.44 ppm confirm the existence of $\text{C}=\text{C}$, indicating the successful synthesis of HepMAM.

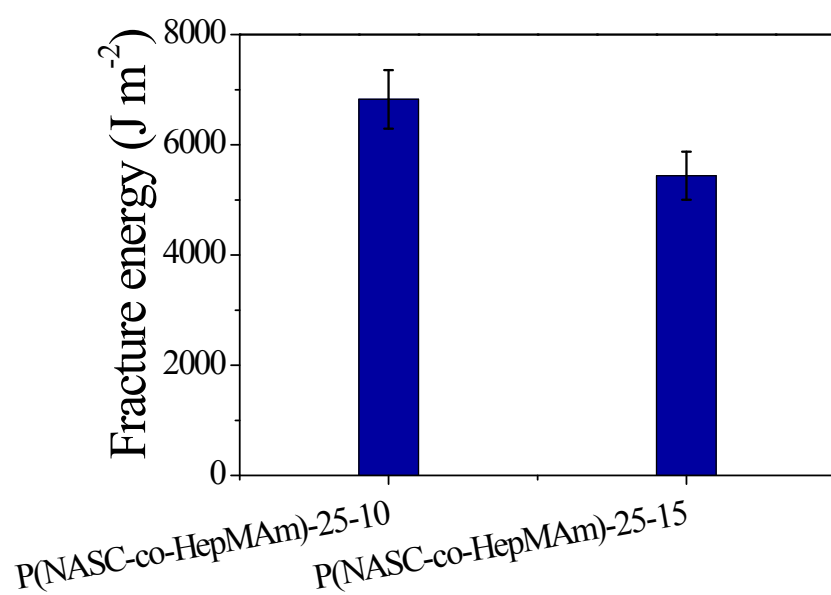
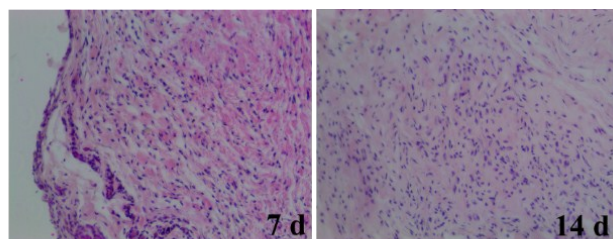


Figure S18. Fracture energies of P(NASC-co-HepMAm)-25-Y hydrogels.

PNASC-25



**P(NASC-co-
HepMAm)-25-15**

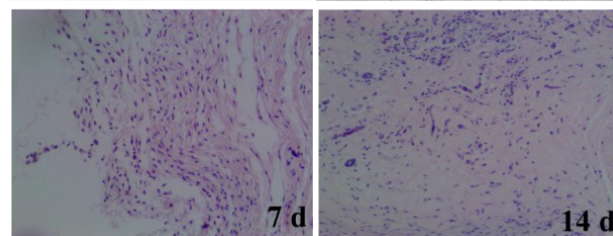


Figure S19. Micrographs of histological sections stained with H&E after 7 days and 14 days *in vivo* implantation of PNASC and P(NASC-co-HepMAm) hydrogels.

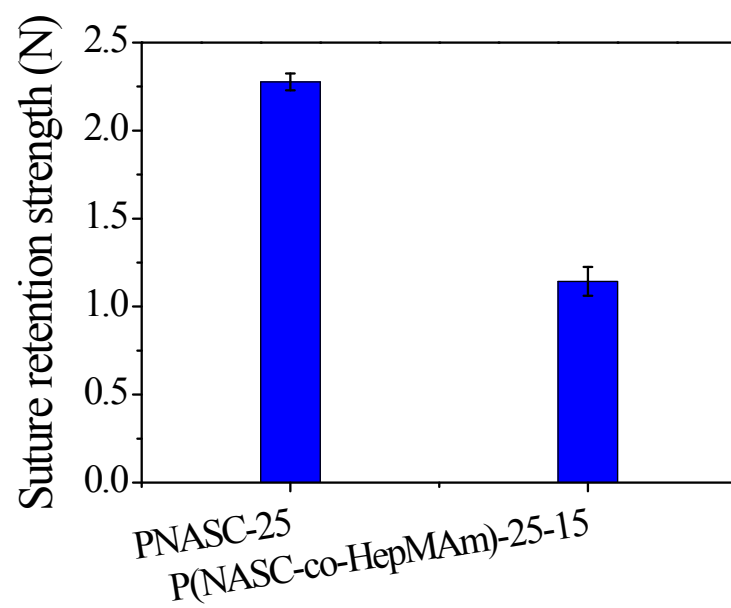


Figure S20. Suture strength of PNASC and P(NASC-co-HepMAm)-25-15 hydrogels.

Movie S1. Lifting the aluminum sheets by a length of PNASC-25 hydrogel line.

Movie S2. Placing a plastic bucket containing 25 L of ethanol on a PMMA board supported by four PNASC-25 hydrogel cylinders.

Movie S3. One person stands on a PMMA board supported by four PNASC-25 hydrogel cylinders.

Movie S4. Transplantation process of a temporary PNASC-25 hydrogel blood vessel substitute.

References

- 1 X. Y. Dai, Y. Y. Zhang, L. M. Gao, T. Bai, W. Wang, Y. L. Cui, W. G. Liu, *Adv. Mater.*, 2015, **27**, 3566.
- 2 H. B. Wang, Y. H. Wu, C. Y. Cui, J. H. Yang, W. G. Liu, *adv. Sci.*, 2018, e1800711.
- 3 H. F. Li, H. B. Wang, D. F. Zhang, Z. Y. Xu, W. G. Liu, *Polymer*, 2018, **153**, 193.
- 4 J. Deng, C. Cheng, Y. Y. Teng, C. X. Nie, C. S. Zhao, *Polym. Chem.*, 2017, **8**, 2266.
- 5 C. E. Ghezzi, B. Marelli, N. Muj, S. N. Nazhat, *Acta Biomater.*, 2012, **8**, 1813.
- 6 F. X. Han, X. L. Jia, D. D. Dai, X. L. Yang, J. Zhao, Y. H. Zhao, Y. B. Fan, X. Y. Yuan, *Biomaterials*, 2013, **34**, 7302.
- 7 D. Huo, G. Liu, Y. Z. Li, Y. X. Wang, G. Guan, M. C. Yang, K. Y. Wei, J. Y. Yang, L. Q. Zeng, G. Li, W. Zeng, C. H. Zhu, *ACS Nano*, 2017, **11**, 10964.